SUPPLEMENTARY MATERIAL

miR-203 and *miR-205* expression patterns identify subgroups of prognosis in cutaneous squamous cell carcinoma

Javier Cañueto *et al.*

PATIENTS, MATERIALS AND METHODS (Supplementary information)

Clinico-epidemiological, pathological and clinical evolution variables of CSCC

We evaluated different clinico-epidemiological, pathological and clinical evolution variables in the cohort of CSCCs studied, which are described in **Supplementary Table S1**. In particular, the clinico-epidemiological variables recorded were: (i) the patients' age; (ii) gender; (iii) clinical history of actinic keratosis, non-melanoma skin cancer and CSCC; (iv) presence of immunosuppression; (v) history of chronic sun exposure; and (vi) tumour location, where we distinguished between head and neck of high risk or poor evolution (including ear, lower lip, temple, nose, eyelid and preauricular region), head and neck of low risk (including the rest of head and neck locations), and trunk and extremities.

Pathological variables: (i) tumour thickness and tumour surface size were measured using hematoxilin-eosin stained samples with the OV100 software (Olympus™) - tumour surface size was the length of the largest diameter of each CSCC in its surface; (ii) the degree of differentiation was classified as good, moderate or poor [32, 33] (iii) the growth pattern was classified as expansive, infiltrative or mixed - the infiltrative growth pattern was considered when the tumour exhibited small nests, rows of cells and/or isolated tumour cells at the periphery of the tumour; the expansive growth pattern was considered when the tumour exhibited a compact growth, with non-disaggregated cells in the invasion front; and the mixed growth pattern was considered when the tumour displayed an expansive growth pattern, but tended to infiltrate any part of the invasion front; (iv) perineural invasion was defined as the infiltration of tumour cells in the perineurum and/or in the nerve itself; (v) lymphovascular invasion was when there were infiltrating tumour cells inside lymphatic and/or blood vessels; (vi) desmoplasia was defined as the thickening of collagen bundles around and inside the tumour that involved at least 30% of the stroma[32] (vii) solar elastosis; (viii) presence of actinic keratosis at diagnosis associated with the tumour (located in the flanking epithelium).

We also considered the variables of poor clinical evolution, such as the occurrence of events associated with a poor prognosis during patient follow up. We studied: (i) local recurrence, considered when the tumour appeared in the same location from where the primary tumour had been removed previously, within the scar or associated with it, two months after surgery or later; (ii) nodal progression; (iii) distant progression when the tumour developed metastases in organs during the clinical follow up; (iv) death due to the CSCC when patients died from a cause related to CSCC; (v) stage of progression, defined by changes in the TNM classification during the follow up according to the 7th edition of the American Joint Committee of Cancer (AJCC) staging guidelines for CSCC; (vi) the existence of any of the previously indicated events associated with a poor clinical evolution during the follow up was also considered as a variable to be evaluated.

In our cohort study, 10 patients were immunosuppressed, 9 of which carried a single tumour. Local recurrence was observed in two cases. One patient displayed nodal progression in this group and had one more tumour, which was not included in this study. This tumour was 15 mm in diameter, moderately differentiated, 2.6 mm in thickness, and did not display perineural invasion (PNI) or lymphovascular invasion (LVI). The likelihood of this tumour causing nodal involvement was very low when compared to the characteristics of the other tumour that was present (poorly differentiated, 28 mm in diameter, 6.3 mm in thickness, with infiltrative growth pattern and PNI). There were no distant metastases in immunosuppressed patients in our cohort. All tumours were excised with as a curative measure.

In situ **hybridization**

Tissue microarray slides were deparaffinised, dehydrated and immersed in 0.2 N HCl for 20 min; then, they were immersed in 0.5% Tween (PBS) solution and fixed in 10% neutral-buffered formalin. Proteinase K (200 mg/ml) digestion was used to treat fixed tissues at

37ºC for 5 min. Following this, the slides were immersed in RNase-free water for 3 min and air-dried. The slides were prehybridized in 65% formamide, 5% SSC, 1% Tween-20, 100 mg/ml yeast RNA at 37º C for 2 hr, followed by hybridization with the probe at 37º C for 24 hr. Oligonucleotide probes complementary to *miR-205* and *miR-203* were purchased from Sigma. The probe sequences were: 5´-CAGACTCCGGTGGAATGAAGGA-3` *(miR-205)* and 5´-CAAGTGGTCCTAAACATTTCAC-3´ *(miR-203).* Both the 5' and 3´ ends were labelled with digoxigenin (DIG). The scrambled probe 5`-AGTCTATGGTATTCAGTACTCA-3` was used as a control. After hybridization the slides were washed in 2% SSC with 0.5% Tween-20 twice for 5 min at room temperature. DIG was identified through a specific antibody conjugated alkaline with phosphatase. This converts the soluble substrate 5-bromo-4-chloro-3'-indolylphosphate (BCIP) into a dark blue water- and alcohol-insoluble precipitate (NBT-BCIP). Finally, the nuclear counterstain was done with *Fast Red*.

Biplot interpretation

The biplot represents patients as points, and variables as vectors on a scattergram as a means of exploring the main characteristics of the data set. The distances among patients - points on the scattergram - are inversely related to their profile similarities, that is, patients close together have similar characteristics. Angles between vectors (variables) indicate the degree of association between variables. Acute angles indicate that the variables are closely related, that is, when a patient displays one of the characteristics he/she also displays the other one and vice versa. The angles between vectors representing the variables and factorial axis estimate the degree of relationship between the variable and the latent dimension, considering that the horizontal axis always provides more information. Variables forming acute angles with the first axis are the most relevant ones, ordering the patients in relation to the most important gradient of disease prognosis,

that is, to classify patients according to the prognosis of the disease. The projections of the patients onto the vector, representing the variables, estimate the expected probability of the characteristic for that patient given his/her combination of disease traits. The length of the vector that represents each variable indicates the discriminating power of the variable in separating out the patients. Shorter vectors are those with the greatest discriminatory power (as long as their information is adequately represented on the plot) [31].

SUPPLEMENTARY FIGURE LEGEND

Supplementary Figure S1. Clusters of CSCC prognosis identified by the logistic biplot. The figure shows cluster 1 (green) as having the best prognosis; cluster 2 as having an intermediate-good prognosis (red) and cluster 3 (blue) as having the worst prognosis. The characteristics of these clusters are shown in Table 1B. GP: Growth pattern; GD: Grade of differentiation; PNI: Perineural Infiltration; DESMO: Desmoplasia. See Supplementary materials and methods for more detailed explanation of the biplot interpretation.

Supplementary Figure S1

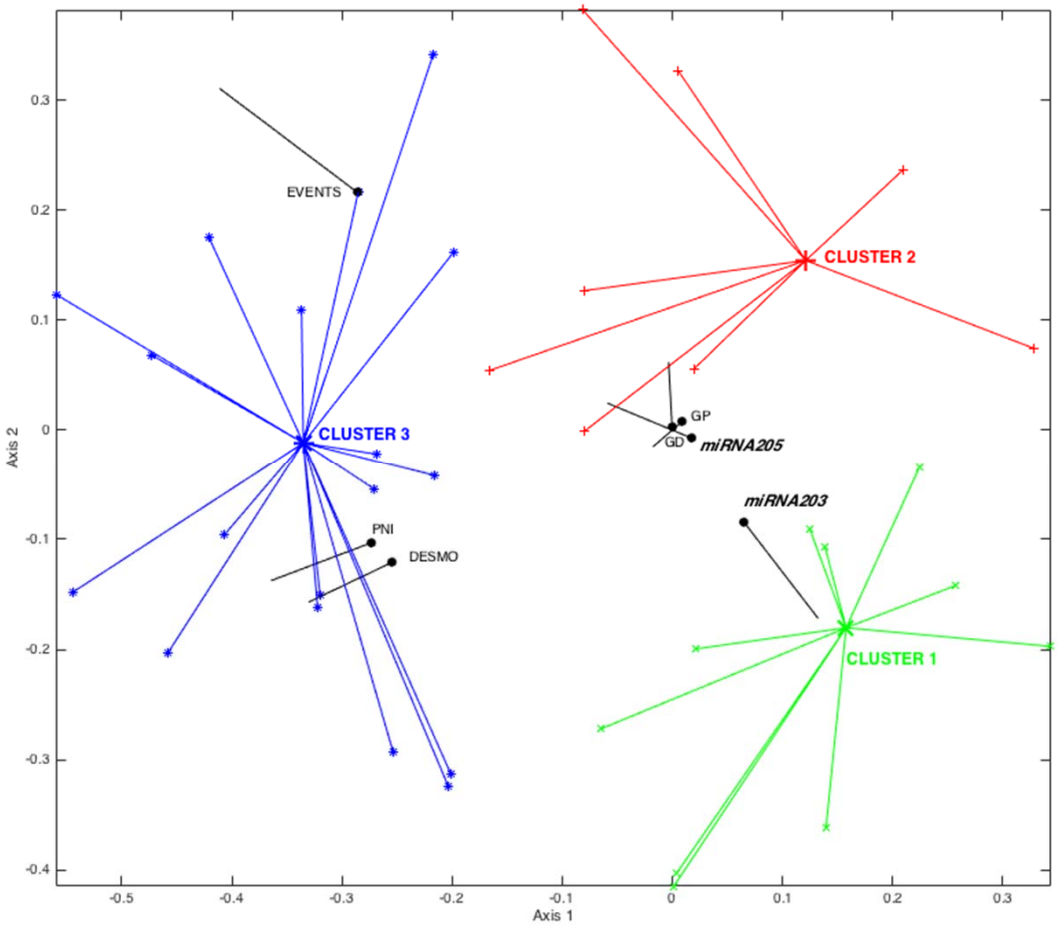

Supplementary Table S1. Descriptive data in the cohort of patients with CSCC.

The table shows the clinico-epidemiological, pathological and clinical evolution characteristics of the study cohort. N: number of cases. SD: standard deviation. M: males. F: females. HN: head and neck. NMSC: Non-melanoma skin cancer. EE: extremities. mm: millimetres. n.a.: not applicable.

Variables			N	Percentage
Clinico-epidemiological Variables	Age (years) (mean (SD)		83.92 (9.63)	n.a.
	Gender		45M/34F	n.a.
	History of actinic keratosis		61	77.2
	History of NMSC		41	51.9
	History of CSCC		37	46.5
	Immunosuppression		9	11.4
	Location	High risk	38	48.1
		Low risk	41	51.9
Pathological Variables	Thickness (mean (SD) in mm)		6.68 (4.611)	n.a.
	Size (mean (SD) in mm)		18.93 (9.96)	n.a.
	Grade of differentiation	Good	25	31.6
		Moderate	37	46.8
		Poor	17	21.5
	Growth pattern	Expansive	26	32.9
		Mixed	17	21.5
		Infiltrative	36	45.6
	Perineural invasión		14	17.7
	Lymphovascular invasión		6	7.6
	Desmoplasia		21	26.6
	Solar elastosis		76	96.2
	Positive margins		0	0
Clinical Evolution Variables	Events of bad prognosis considered globally		12	15.2
	Local recurrence		4	5.1
	Nodal progression		10	12.7
	Metastasis		1	1.3
	Changes in the stage of progression (TNM)		10	12.7
	Death		5	5.1

Supplementary Table S2. Associations between different tumour features of CSCC. The table shows associations among pathological traits that were statistically significant (red) or showed statistical trend (blue). N: number of cases. N.S.: non-significant. mm: millimetres. Red: significant *P* values. Blue: statistical tendency.

		Growth Pattern			
		Expansive	**Mixed**	**Infiltrative**	***P* value**
Grade of Differentiation (N)	**Good**	13	9	3	0.00001
	Moderate	10	8	19	
	Poor	3	0	14	
Desmoplasia (N)	**Yes**	2	3	16	0.003
	No	24	14	20	
Perineural Invasion (N)	**Yes**	0	1	13	0.0001
	No	26	16	23	
Tumour Thickness (median in mm)		18 (10)	18 (7)	20 (10)	0.001
Tumour Size (median in mm)		3.5 (4.25)	5 (3.95)	6.25 (7)	N.S.
		Grade of Differentiation			
		Good	**Moderate**	**Poor**	***P* value**
Desmoplasia (N)	**Yes**	3	11	7	0.092
	No	22	26	10	
Perineural Invasion (N)	**Yes**	1	7	6	0.032
	No	24	30	11	
Tumour Thickness (median in mm)		4 (2.63)	6 (4.5)	6 (6.25)	0.023
Tumour Size (median in mm)		19 (9)	15 (8)	20 (10)	N.S.
		Perineural Invasion			
		Yes		**No**	***P* value**
Tumour Thickness (median in mm)		8 (7)		5 (4.60)	0.007
Tumour Size (median in mm)		20.5 (11.25)		15.50 (7.75)	0.069
		Desmoplasia			
		Yes		**No**	***P* value**
Perineural Invasion (N)	**Yes**	9		5	0.00001
	No	12		53	

Supplementary Table S3. List of miRNAs differentially expressed in skin cancer cell lines with different grade of aggressiveness. A) List of 45 miRNAs most differentially expressed in non-malignant versus squamous CSCC cell lines. **B**) List of 43 miRNAs most differentially expressed between squamous CSCC and spindle CSCC cell lines. These lists of miRNAs are represented in the heatmaps on Figure1A and 1B, respectively.

A. Non-malignant squamous / Squamous CSCC ratio				
miRNA		**RMA signal (log2 ratio)**		**RMA signal (decimal ratio)**
hsa-miR-671-3p/mmu-miR-671-3p/rno-miR-671	↑	1.20	↑	2.64
hsa-let-7g*/mmu-let-7g*	↑	1.17	↑	2.15
hsa-miR-203/mmu-miR-203/rno-miR-203	↑	1.15	↑	2.07
hsa-miR-19a*/mmu-miR-19a*	↑	1.14	↑	2.00
hsa-miR-200c/mmu-miR-200c/rno-miR-200c	↑	1.12	↑	1.95
mmu-miR-34b-5p/rno-miR-34b	↑	1.11	↑	1.66
hsa-miR-140-5p/mmu-miR-140/rno-miR-140	↑	1.11	↑	1.74
hsa-miR-194/mmu-miR-194/rno-miR-194	↑	1.10	↑	1.62
hsa-miR-205/mmu-miR-205/rno-miR-205	↑	1.10	↑	1.86
hsa-miR-224/mmu-miR-224/rno-miR-224	↑	1.09	↑	1.49
hsa-miR-19a/mmu-miR-19a/rno-miR-19a	↓	0.90	↓	0.50
hsa-miR-182/mmu-miR-182/rno-miR-182	↓	0.90	↓	0.51
hsa-miR-26a/mmu-miR-26a/rno-miR-26a	↓	0.89	↓	0.51
hsa-miR-146a/mmu-miR-146a/rno-miR-146a	↓	0.89	↓	0.56
hsa-miR-29c/mmu-miR-29c/rno-miR-29c	↓	0.89	↓	0.53
mmu-let-7d/rno-let-7d	↓	0.89	↓	0.46
mmu-miR-706	↓	0.89	↓	0.47
hsa-let-7a/mmu-let-7a/rno-let-7a	↓	0.89	↓	0.46
hsa-miR-31/mmu-miR-31/rno-miR-31	↓	0.88	↓	0.40
mmu-let-7g	↓	0.88	↓	0.42
hsa-miR-142-5p/mmu-miR-142-5p/rno-miR-142-5p	↓	0.88	↓	0.53
hsa-miR-16/mmu-miR-16/rno-miR-16	↓	0.88	↓	0.42
hsa-miR-365/mmu-miR-365/rno-miR-365	↓	0.88	↓	0.48
hsa-miR-15b/mmu-miR-15b/rno-miR-15b	↓	0.88	↓	0.43
hsa-miR-23a/mmu-miR-23a/rno-miR-23a	↓	0.88	↓	0.38
hsa-miR-20a/mmu-miR-20a/rno-miR-20a	↓	0.87	↓	0.40
hsa-miR-801/mmu-miR-801	↓	0.87	↓	0.43
mmu-miR-685	↓	0.87	↓	0.44
mmu-miR-106a	↓	0.85	↓	0.36
hsa-miR-142-3p/mmu-miR-142-3p/rno-miR-142-3p	↓	0.85	↓	0.44
hsa-miR-106b/mmu-miR-106b/rno-miR-106b	↓	0.85	↓	0.34
hsa-miR-668/mmu-miR-668	↓	0.85	↓	0.35
hsa-let-7e/mmu-let-7e/rno-let-7e	↓	0.85	↓	0.27
hsa-miR-9*/mmu-miR-9*/rno-miR-9*	↓	0.85	↓	0.41
hsa-miR-21/mmu-miR-21/rno-miR-21	↓	0.84	↓	0.24
mmu-miR-690	↓	0.84	↓	0.22
hsa-miR-125b/mmu-miR-125b-5p/rno-miR-125b-5p	↓	0.84	↓	0.28
hsa-miR-22/mmu-miR-22/rno-miR-22	↓	0.83	↓	0.29
hsa-miR-19b/mmu-miR-19b/rno-miR-19b	↓	0.83	↓	0.28
mmu-miR-207/rno-miR-207	↓	0.83	↓	0.24
hsa-miR-222/mmu-miR-222/rno-miR-222	↓	0.82	↓	0.25
hsa-miR-221/mmu-miR-221/rno-miR-221	↓	0.81	↓	0.27
hsa-miR-193a-3p/mmu-miR-193/rno-miR-193	↓	0.81	↓	0.27
hsa-miR-29a/mmu-miR-29a/rno-miR-29a	↓	0.79	↓	0.18
hsa-miR-29b/mmu-miR-29b/rno-miR-29b	↓	0.78	↓	0.16

B. Squamous CSCC / Spindle CSCC ratio				
miRNA		RMA signal (log2 ratio)		RMA signal (decimal ratio)
hsa-miR-205/mmu-miR-205/rno-miR-205	↑	1.31	↑	4.51
hsa-miR-200b/mmu-miR-200b/rno-miR-200b	↑	1.25	↑	3.33
hsa-miR-141/mmu-miR-141/rno-miR-141	↑	1.25	↑	3.33
hsa-miR-106b/mmu-miR-106b/rno-miR-106b	↑	1.24	↑	4.04
hsa-miR-200a/mmu-miR-200a/rno-miR-200a	↑	1.24	↑	2.98
hsa-miR-200c/mmu-miR-200c/rno-miR-200c	↑	1.20	↑	2.47
hsa-miR-31/mmu-miR-31/rno-miR-31	↑	1.20	↑	3.75
hsa-miR-23a/mmu-miR-23a/rno-miR-23a	↑	1.20	↑	3.67
mmu-miR-466f-3p	↑	1.19	↑	3.27
hsa-miR-20a/mmu-miR-20a/rno-miR-20a	↑	1.19	↑	3.06
hsa-miR-22/mmu-miR-22/rno-miR-22	↑	1.18	↑	3.12
hsa-miR-21/mmu-miR-21/rno-miR-21	↑	1.18	↑	3.95
hsa-miR-222/mmu-miR-222/rno-miR-222	↑	1.18	↑	3.07
hsa-miR-183/mmu-miR-183/rno-miR-183	↑	1.17	↑	2.45
hsa-miR-182/mmu-miR-182/rno-miR-182	↑	1.16	↑	2.46
hsa-miR-30b/mmu-miR-30b/rno-miR-30b-5p	↑	1.16	↑	2.44
hsa-miR-16/mmu-miR-16/rno-miR-16	↑	1.15	↑	2.52
hsa-miR-30c/mmu-miR-30c/rno-miR-30c	↑	1.14	↑	2.23
hsa-miR-30a/mmu-miR-30a/rno-miR-30a	↑	1.14	↑	2.29
hsa-miR-146a/mmu-miR-146a/rno-miR-146a	↑	1.13	↑	1.86
hsa-miR-18a/mmu-miR-18a/rno-miR-18a	↑	1.13	↑	1.98
hsa-miR-146b-5p/mmu-miR-146b	↑	1.11	↑	1.73
hsa-miR-301a/mmu-miR-301a/rno-miR-301a	↑	1.11	↑	1.89
mmu-miR-20b	↑	1.10	↑	1.75
hsa-miR-24-2*/mmu-miR-24-2*/rno-miR-24-2*	↑	1.10	↑	1.65
hsa-miR-19b/mmu-miR-19b/rno-miR-19b	↑	1.10	↑	2.02
mmu-miR-466e-5p	↑	1.10	↑	1.68
mmu-miR-20b*/rno-miR-20b-3p	↑	1.10	↑	1.55
hsa-miR-200a*/mmu-miR-200a*	↑	1.10	↑	1.57
hsa-miR-31*/mmu-miR-31*	↑	1.10	↑	1.70
hsa-miR-34a/mmu-miR-34a/rno-miR-34a	↑	1.10	↑	1.73
hsa-miR-24-1*/mmu-miR-24-1*/rno-miR-24-1*	↑	1.09	↑	1.75
hsa-miR-135b/mmu-miR-135b/rno-miR-135b	↑	1.09	↑	1.56
hsa-miR-27b/mmu-miR-27b/rno-miR-27b	↑	1.09	↑	1.88
mmu-miR-34b-5p/rno-miR-34b	↓	0.89	↓	0.58
mmu-miR-382*	↓	0.89	↓	0.52
mmu-miR-455	↓	0.89	↓	0.57
mmu-miR-433*	↓	0.87	↓	0.43
hsa-miR-199a-5p/mmu-miR-199a-5p/rno-miR-199a	↓	0.87	↓	0.50
mmu-miR-199b*	↓	0.87	↓	0.50
hsa-miR-199a-3p/hsa-miR-199b-3p/mmu-miR-199a	↓	0.84	↓	0.42
hsa-miR-181a/mmu-miR-181a/rno-miR-181a	↓	0.83	↓	0.38
hsa-miR-143/mmu-miR-143/rno-miR-143	↓	0.81	↓	0.35

Supplementary Table S4: Quantification of *miR-203* and *miR-205* expression in human CSCC. The table shows the degree of expression in differentiated and undifferentiated areas, and in the invasion front. N: number of cases.

miRNA expression				
	miR-203			
		Differentiated areas	***Undifferentiated***	***P* value**
	Absent and scarce (N)	33	36	**0.014**
	Moderate and intense (N)	28	10	
	miR-205			
		Differentiated areas	***Undifferentiated***	***P* value**
	Absent and scarce (N)	38	11	**< 0.0001**
	Moderate and intense (N)	8	27	
	Front of invasion			
		miR-203	***miR-205***	***P* value**
	Absent and scarce (N)	33	19	**0.0008**
	Moderate and intense (N)	11	29	

Supplementary Table S5. Associations of *miR-205* and *miR-203* genral expression with different characteristics of CSCC. **A**) Associations of clinico-pathological tumour traits and *miR-205* and *miR-203* expression. **B**) Associations of expression of *miR-205* and *miR-203* in the invasion front with the presence of different tumour traits. **C**) Associations of *miR-205* and *miR-203* and epithelial markers, E-CADHERIN and P63 expression. N.S.: non-significant. I.R.: interquartile range. Red: significant *P* values. Blue: statistical trend.

A.	**CLINICO-PATHOLOGICAL TUMOUR TRAITS AND GLOBAL EXPRESSION OF *miR-205* AND *miR-203***						
		miR-203			***miR-205***		
		Expression	**No expression**	***P* value**	**Expression**	**No expression**	***P* value**
Desmoplasia	Yes	4	17	**0.05**	14	7	**0.064**
	No	25	33		25	33	
Growth pattern	Expansive	11	15	N.S.	6	20	**0.003**
	Mixed	4	13		9	8	
	Infiltrative	14	22		24	12	
Perineural invasion	Yes	3	11	N.S.	11	3	**0.016**
	No	26	39		28	37	
Thickness (Median (IR))		6 (8.25)	6(3)	N.S.	6 (7)	5.75 (2.88)	**0.023**
Surface (Median (IR))		21 (10.75)	20 (11.50)	N.S.	20 (11)	20 (8.5)	N.S.
B.	**PATHOLOGICAL TUMOUR TRAITS AND EXPRESSION OF *miR-205* AND *miR-203* IN THE FRONT OF INVASION**						
		miR-203			***miR-205***		
		Expression	**No expression**	***P* value**	**Expression**	**No expression**	***P* value**
Growth pattern	Expansive	7	4	**0.001**	4	9	**0.026**
	Mixed	3	9		6	4	
	Infiltrative	1	20		19	6	
Desmoplasia	Yes	0	12	**0.086**	9	6	N.S.
	No	11	21		20	13	
Perineural invasion	Yes	0	11	**0.027**	10	2	**0.061**
	No	11	22		19	17	
Thickness (Median (IR))		4 (2.75)	6.5 (6.5)	**0.003**	6.5 (7.5)	5.75 (2.38)	N.S.
C.	**EPITHELIAL MARKERS AND GLOBAL EXPRESSION OF *miR-205* and *miR-203***						
		miR-203			***miR-205***		
		Expression	**No expression**	***P* value**	**Expression**	**No expression**	***P* value**
E-CADHERIN	Expression	21	30	N.S.	24	27	N.S
	No expression	8	20		15	13	
P63	Expression	8	29	**0.009**	27	10	**0.0001**
	No expression	21	21		12	30	